

Nanostructured Films Made from Zwitterionic Phosphorylcholine Diblock Copolymer Systems

Ledilege C. Porto,^{†,‡} Karim Aissou,[†] Cristiano Giacomelli,[§] Thierry Baron,[⊥] Cyrille Rochas,[†] Isabelle Pignot-Paintrand,[†] Steven P. Armes,^{||} Andrew L. Lewis,[○] Valdir Soldi,[‡] and Redouane Borsali^{*,†}

[†]Centre de Recherches sur les Macromolécules Végétales (CERMAV-CNRS), affiliated with Joseph Fourier University and ICMG FR 2607, BP53, 38041 Grenoble Cedex 9, France

[‡]Departamento de Química, Universidade Federal de Santa Catarina, 88040-900 Florianópolis, SC, Brazil

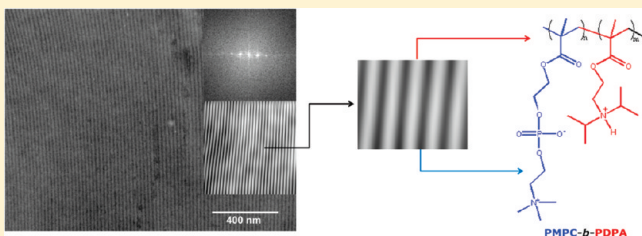
[§]Departamento de Química, Universidade Federal de Santa Maria, Av. Roraima 1000, 97105-900, Santa Maria, RS, Brazil

[⊥]Laboratoire des Technologies de la Microélectronique (LTM-CNRS), 17 Rue des Matyrs, 38052 Grenoble, cedex 9, France

^{||}Department of Chemistry, University of Sheffield, Brook Hill, Sheffield, South Yorkshire, S3 7HF, U.K.

[○]Biocompatibles U.K. Ltd., Chapman House, Farnham Business Park, Weydon Lane, Farnham, Surrey, GU9 8QL, U.K.

ABSTRACT: The morphology of an AB diblock copolymer comprising a highly biocompatible poly[2-(methacryloyloxy)ethyl phosphorylcholine] block and a pH-sensitive poly[2-(diisopropylamino)ethyl methacrylate] block (PMPC₃₀-*b*-PDPA₆₀) was analyzed using SAXS and (S)TEM. PMPC₃₀-*b*-PDPA₆₀ films cast from ethanol solution at room temperature exhibit a thermodynamically quasi-stable cylindrical morphology, which undergoes an order–order transition upon thermal annealing at 170 °C: the resulting lamellar structure coexists with a minor proportion of cylinders organized into a hexagonal compact phase. In contrast, copolymer films cast from methanol do not undergo the same morphological transition. Instead, short-range liquid-like structures are obtained regardless of the annealing processes. Finally, direct self-assembly to form a lamellar morphology *at room temperature* can be achieved by solvent-casting from aqueous solution at pH 4.



INTRODUCTION

Block copolymers have been utilized to fabricate nanomaterials via a “bottom-up” process in which a finite number of elementary building-blocks (macromolecular chains) self-assemble hierarchically.^{1,2} Covalent linkage between two or more incompatible polymer chains limits their phase separation to length scales that are predefined by the chain dimensions.³ Thus, each block resides in its own phase while remaining covalently attached to the other; the coexistence of short-range attractive and long-range repulsive forces in such a configuration leads to the formation of ordered domains.⁴

In the rapidly expanding field of macromolecular self-assembly, it is now possible to design next-generation copolymer-based nanostructured thin films that simultaneously feature long-range order, stimulus-responsiveness and spontaneously form versatile supramolecular structures.^{5,6} In this context, the poly[2-(methacryloyloxy)ethyl phosphorylcholine]-*block*-poly[2-(diisopropylamino)ethyl methacrylate] (PMPC-*b*-PDPA) copolymer is a very attractive functional building block. PMPC is a highly hydrophilic, biomimetic polymer that finds widespread biomedical and cosmetic applications due to its excellent biocompatibility and nonfouling properties.^{7–9} Meanwhile, PDPA is a pH-responsive polymer due to its pendent tertiary amine groups, which can act as hydrogen-bonding sites in the formation of supramolecular structures.¹⁰ As a weak polybase, it can form (poly)electrolyte complexes with antagonist weak acids.¹¹ These

characteristics suggest that PDPA—and structurally related poly[2-(dialkylamino)ethyl methacrylates] in general—can be used to prepare stable vesicles and micelles for the encapsulation of hydrophobic or hydrophilic molecules,^{12–16} with high loading capacities being achieved via specific acid/base interactions.¹⁷ Hybrid organic–inorganic nanostructured materials in which metallic nanoparticles are distributed selectively within the PDPA microdomains have also been prepared.¹⁸

From the perspective of thin film formation, PMPC-*b*-PDPA copolymers are of broad potential interest in the field of functional (bio)nanomaterials engineering. We anticipated that this system would exhibit a more complex phase diagram compared to classical systems because of the additional functionality of each block (i.e., the zwitterionic nature of PMPC, and the pH-sensitivity, hydrogen-bonding capability, and acid–base interactions that are characteristic of PDPA), which can exert a subtle influence over the balance of driving forces during the segregation process.¹⁹

In this study, well-defined nanostructured thin films are prepared for the first time from a PMPC-*b*-PDPA diblock copolymer simply by solvent casting. These copolymer films undergo order–order morphology transitions upon solvent and

Received: December 27, 2010

Revised: January 10, 2011

Published: March 02, 2011

thermal annealing, as corroborated by scanning and transmission electron microscopy ((S)TEM) and small-angle X-ray scattering (SAXS) techniques.

EXPERIMENTAL METHODS

Materials and Sample Preparation. The PMPC₃₀-*b*-PDPA₆₀ (here and throughout the text subscripts refer to the mean degrees of polymerization of each block) diblock copolymer ($M_n = 21\,000$ g/mol, $M_w/M_n = 1.27$; DPA volume fraction = 0.57) was synthesized via sequential monomer addition using ATRP as previously described by Ma et al.²⁰

Preparation of Self-Assembled Diblock Copolymer Thin Films. The PMPC₃₀-*b*-PDPA₆₀ diblock copolymer films were cast from 10% (w/v) ethanol, methanol, or dilute acidic solution (pH 4), which were initially stirred for 24 h followed by slow solvent evaporation at ambient temperature. After complete removal of the solvent, the samples were annealed under vacuum for 24 h at temperatures ranging from 25 to 170 °C.

Scanning and Transmission Electron Microscopy ((S)TEM). For TEM imaging, part of the annealed film were embedded in epoxy resin, which was then cured for 72 h at 60 °C. Thin sections of 70 nm nominal thickness were obtained using a UC6 Leica ultramicrotome and a Diatome diamond knife at room temperature. Sections were collected on carbon-coated copper grid. Electron microscopy observations were conducted with a CM200 Philips transmission electron microscope at an accelerating voltage of 80 kV and with a Zeiss ultra 55 FEG-scanning electron microscope operating at an accelerating voltage of 10 kV using a STEM detector.

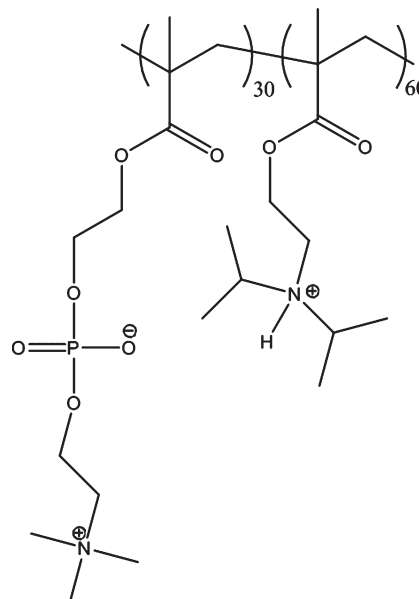
Small-Angle X-ray Scattering (SAXS). SAXS measurements were performed at the beamline BM02, European Synchrotron Radiation Facility (ESRF, Grenoble, France)²¹ and also at the D11A-SAXS beamline of the Brazilian Synchrotron Light Laboratory (LNLS, Campinas, SP, Brazil). At the BM02 beamline, copolymer films were placed in cylindrical capillaries of 1.5 mm internal diameter, the measurements were carried out at an incident energy of 16 keV and scattered intensities were recorded at distance of 1.60 m using a two-dimensional CCD detector with an active area of 44 cm² (Ropper Scientific). At the D11A beamline, measurements were carried out at 8.6 keV and scattered intensities were recorded using a two-dimensional CCD Mar detector with an active area of 16 cm² (Rayonix) at distance of 1.60 m. Depending on the beamline used the azimuthal integration was done using the FIT2D software developed by Hammersley²² or with the Bm2img software developed on BM02, see reference²³ for more details. The 2D pictures were corrected for dark current, distortions of the detector and normalized to the transmission and beam's intensity.

RESULTS AND DISCUSSION

The PMPC₃₀-*b*-PDPA₆₀ block copolymer system (21 kg/mol, $M_w/M_n = 1.27$) used in this study is presented on the Scheme 1. The relative volume fractions, f , of the two individual blocks were estimated to be 0.43 and 0.57 for PMPC ($d = 1.30$ g·cm⁻³)²⁴ and PDPA ($d = 1.33$ g·cm⁻³),²⁵ respectively.

High and low magnification TEM images for PMPC₃₀-*b*-PDPA₆₀ thin films, annealed at 170 °C for 1 day, are presented in Figure 1. The thermal annealing process removes the residual ethanol solvent and minimizes possible surface-induced nonequilibrium effects, thus increasing the probability of reaching morphologies in thermodynamic equilibrium. It is noteworthy that the TEM images were acquired without using any staining agents. Consequently, the PMPC-*b*-PDPA intrinsic electron density contrast due to the phosphorus atoms in the PMPC chains yields to PMPC domains darker than PDPA ones. The

Scheme 1. Schematic Representation of Poly-[2-(methacryloyloxy)ethyl phosphorylcholine]-*block*-poly-[2-(diisopropylamino)ethyl methacrylate] (PMPC-*b*-PDPA) block copolymer



micrograph in Figure 1a exhibits an exceptional region (more than $4.5 \times 4.0 \mu\text{m}^2$) where a defect-free alternation of PMPC-rich and PDPA-rich nanodomains is observed. The high degree of organization and long-range order which are normally considered essential for most thin film applications¹ are clearly evident in this sample. Figure 1b shows a TEM image which is a high magnification of the strip pattern observed in Figure 1a. The long-range average in-plane periodicity is confirmed by Fast Fourier Transformation (FFT) analysis associated with the image (see inset) on which two main Bragg peaks and higher-order reflections are clearly evident. From this FFT, a domain spacing d of 33.9 nm was extracted. This interdomain spacing roughly corresponds to a highly stretch configuration of chains.

The block copolymer films produced during this study were also investigated using the scanning transmission electron microscopy (STEM) technique. As opposed to TEM micrographs, the STEM image presented in Figure 2 reveals the coexistence of two distinct phases for the same annealing conditions (1 day at 170 °C). The presence of a minor phase exhibiting a hexagonal symmetry in the film (see inset) induces undulations of the PMPC/PDPA interfaces in the dominant phase made of parallelly oriented cylinders or vertically oriented lamella.

Synchrotron SAXS experiments were performed in order to further examine the ordered phases originating from the self-assembly of the PMPC₃₀-*b*-PDPA₆₀ at a large scale ($100 \times 100 \mu\text{m}^2$) compared to microscopy technique. SAXS profiles recorded at room temperature for the PMPC₃₀-*b*-PDPA₆₀ copolymer films cast from an ethanol solution and annealed at different temperatures are shown in Figure 3. For the sample annealed 1 day at 170 °C, the SAXS profile reveals a mixture of two different morphologies in the thin film which is in accordance with the Figure 2. The more reflective one, having a first order peak located at $q^* = 0.19 \text{ nm}^{-1}$ and higher-order peaks observed at relative positions of $2q^*$ and $3q^*$, corresponds to a lamellar morphology with a $d = (2\pi)/(q^*) = 33.0 \text{ nm}$. The other

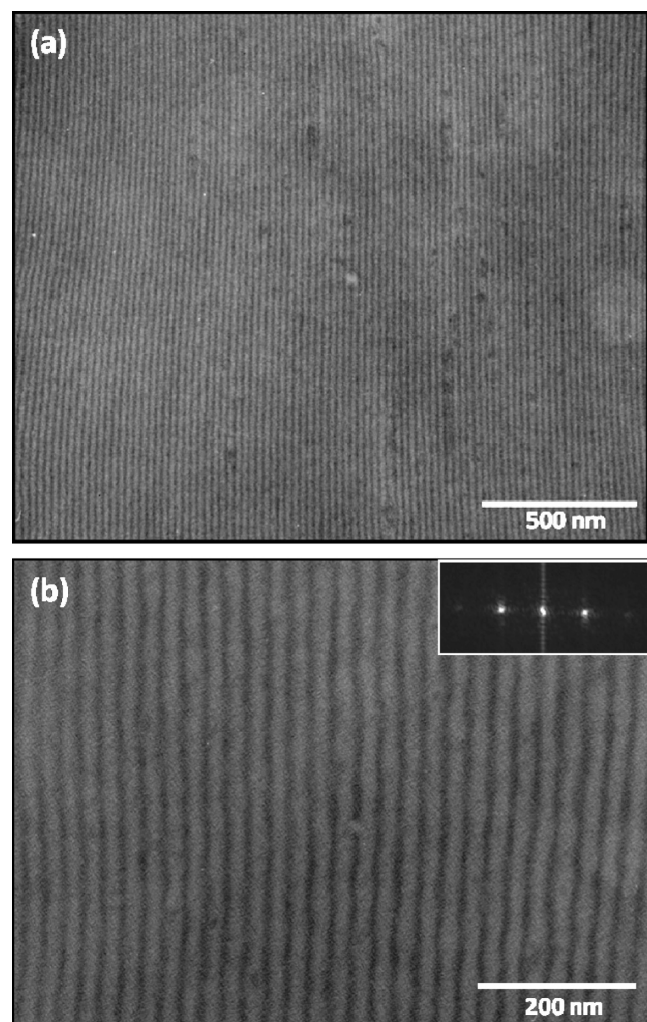


Figure 1. (a and b) TEM images of thin sections of PMPC₃₀-*b*-PDPA₆₀ copolymer films cast from ethanol and subsequently annealed at 170 °C for 1 day to produce strip patterns. The inset shows the corresponding fast Fourier transform of higher magnification image with two orders of Bragg peaks arising from long-range order. Dark regions correspond to the more electron-dense PMPC domains.

one presents only a single broad peak at $q^{**} = 0.13 \text{ nm}^{-1}$. These results suggest that the strip pattern, with a d -spacing of 33.9 nm, observed on TEM and STEM images are alternations of lamella. Moreover, we expect that the single peak at $q^{**} = 0.13 \text{ nm}^{-1}$ is correlated with the phase having a hexagonal symmetry noticed in Figure 2.

The copolymer nanostructure examined before annealing displays a different SAXS profile. In this case, the less reflective phase is the lamellar morphology which is confirmed by the presence of a main peak, q^* , at 0.19 nm^{-1} and a higher-order peak at $q/q^* = 3$ while the more reflective phase presents a first-order peak at $q^{**} = 0.13 \text{ nm}^{-1}$ and also two secondary maxima at relative positions $(3)^{1/2}q^{**}$ and $(7)^{1/2}q^{**}$. The series of scattering peaks following the sequence $q/q^* = 1:(3)^{1/2}:(7)^{1/2}$ is ascribed to cylindrical domains arranged in a hexagonal compact phase with an interdomain spacing, d , about 55.8 nm ($d = (2\pi)/(q^*) \times (4/3)^{1/2}$). Since the volume fraction of PDPA is 0.57, a lamellar morphology should be stable at room temperature. Therefore, the phase transition observed under temperature occurs from a thermodynamically quasi-stable cylindrical morphology, which was formed via

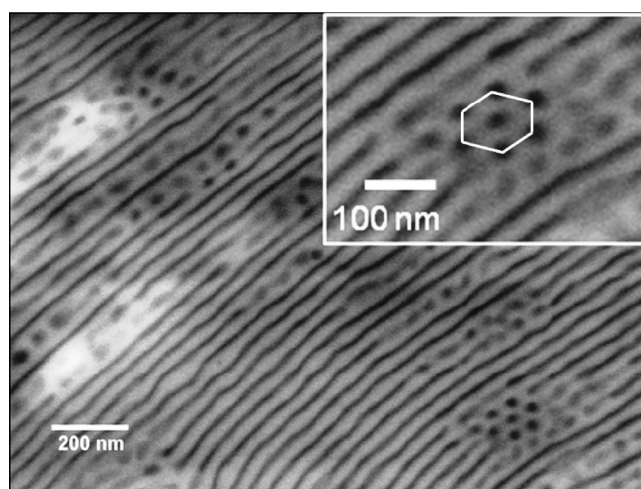


Figure 2. STEM images of a thin section of a copolymer PMPC₃₀-*b*-PDPA₆₀ film cast from ethanol and subsequently annealed at 170 °C for 24 h in which a lamellar and a hexagonal compact phases coexist. Inset on the right shows a higher magnification image depicting a hexagonal arrangement of the minor phase.

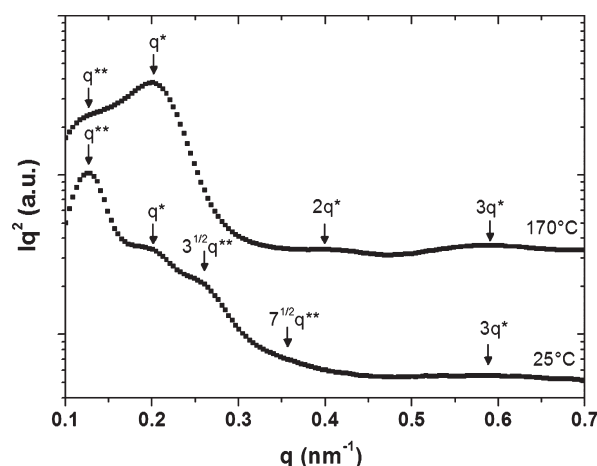


Figure 3. Variation of Iq^2 vs q for PMPC₃₀-*b*-PDPA₆₀ films cast from 10% w/v ethanol both room temperature and after annealing at 170 °C for 24 h, as indicated. These SAXS patterns clearly evidence the coexistence of lamellar and cylindrical morphologies.

casting the block copolymer solutions with a solvent having more affinity with PDPA, to a stable lamellar morphology.

At this stage, we have examined the structure of copolymer films obtained from other cast solvents such as methanol or dilute acidic solution (pH 4.0). We wished to verify the stability of the two coexisting morphologies obtained from ethanol, which are expected to be sensitive to the choice of solvent since only one phase should be thermodynamically stable. The physical behavior of the solvent can also influence the conformation of the block copolymer in the ordered state. Besides, micellar structures may exist when selective solvents (i.e., a solvent that is thermodynamically good for one block but a poor solvent for the other block) are used.^{1,3,26,27} Interestingly, the same morphological transition did not occur upon annealing when the copolymer films were cast from methanol (Figure 4). Each SAXS pattern exhibits two broad reflections at relative spacing q^* and $(3)^{1/2}q^*$

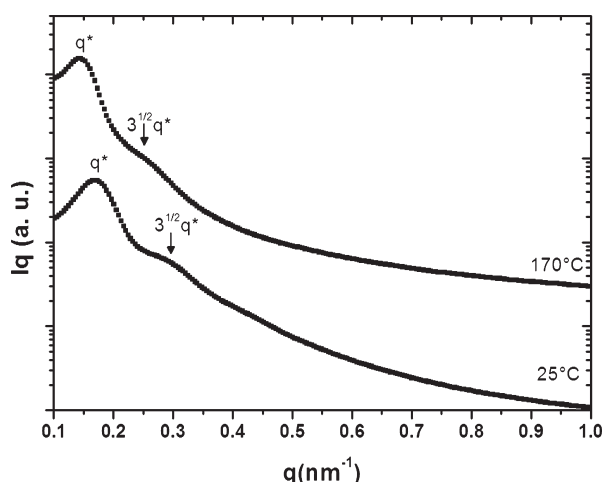


Figure 4. Variation of Iq vs q for PMPC₃₀-*b*-PDPA₆₀ films cast from 10% w/v methanol both room temperature and after annealing at 170 °C for 24 h, as indicated. These SAXS patterns reveal for both temperatures that domains are poorly organized.

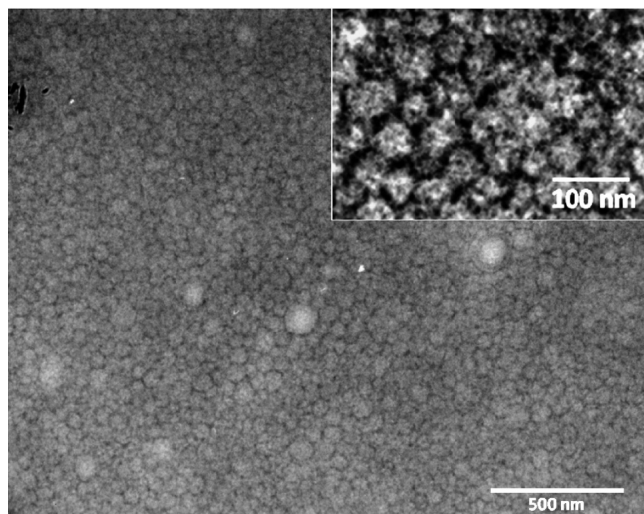


Figure 5. TEM images of thin sections of a PMPC₃₀-*b*-PDPA₆₀ copolymer film cast from methanol and subsequently annealed at 170 °C for 1 day to produce a short-range liquid-like structure.

which indicate that domains are packed in a short-range liquid-like structure. The broad peak at $(3)^{1/2}q^*$ could be a superposition of the other order reflections. Before annealing, the first intensity maximum at $q^* = 0.17 \text{ nm}^{-1}$ corresponds to a periodicity of 36.9 nm. Upon annealing, this peak shifts to lower q values and the maximum is observed at $q^* = 0.14 \text{ nm}^{-1}$, reflecting a periodicity of 44.5 nm, which is fully supported by the TEM images shown in Figure 5. The low resolution of the discrete scattering associated with the structures in Figure 4 (in which higher order peaks cannot be identified) is attributed to a lack of self-organization within this film. In fact, the image depicted in Figure 5 reveals rather poor positional correlation between nanodomains, whose the average size conforms to the dimensions of PDPA-core micelles formed by direct dissolution of the PMPC₃₀-*b*-PDPA₆₀ copolymer in methanol prior to film formation.

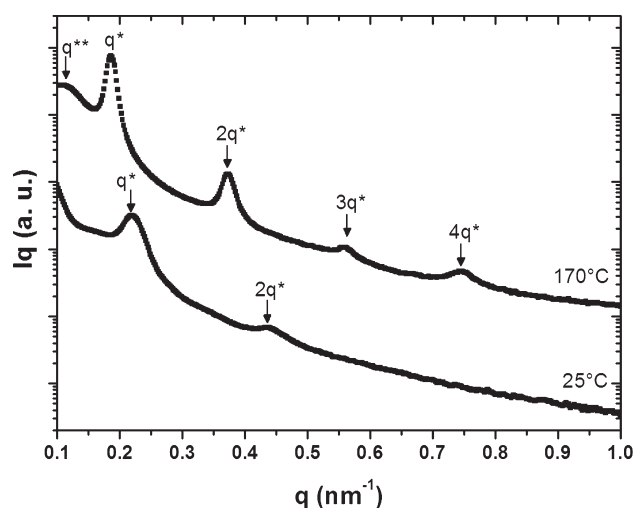


Figure 6. Variation of Iq vs q for PMPC₃₀-*b*-PDPA₆₀ films cast from dilute acidic solution both room temperature and after annealing at 170 °C for 24 h, as indicated. The SAXS pattern obtained at room temperature indicates that domains are organized lamellar structure. Upon annealing, the lamellar phase becomes significantly more organized and supplementary peak noted q^{**} appears plus to peaks relative to a lamellar phase.

On the basis of the results reported above, it is clear that the copolymer film formation strongly depends on the polymer–solvent interactions. Hence we elected to investigate the nanostructure of PMPC₃₀-*b*-PDPA₆₀ films cast from dilute acidic solution. PMPC-*b*-PDPA copolymer chains can be molecularly dissolved in dilute acidic solution due to the protonation of the pH-sensitive PDPA block, which has a pK_a of 5.7–6.6 depending on the solution conditions.¹³ Therefore, copolymer films cast from mildly acidic solution (pH 4.0) at room temperature comprise a molecularly dissolved diblock copolymer consisting of a zwitterionic PMPC block and a cationic PDPA block. Under these conditions, the copolymer chains self-organize directly to produce a lamellar morphology, *without requiring any thermal annealing*. As revealed by the SAXS data in Figure 6, the lamellar phase prior to annealing is characterized by two orders of reflections at $q/q^* = 1:2$. Upon annealing, the lamellar structure becomes significantly more organized: four sharp scattering peaks with relative wave-vector ratios $q/q^* = 1:2:3:4$ become evident, as does the shoulder noted q^{**} and attributed to the cylindrical morphology previously observed by SAXS and TEM in the diblock copolymer films cast from ethanol. Before annealing, the first intensity maximum at $q^* = 0.22 \text{ nm}^{-1}$ corresponds to a periodicity of 28.5 nm relative to the lamellar structure. Nevertheless, the first order peak is reduced to $q^* = 0.19 \text{ nm}^{-1}$ upon annealing at 170 °C which corresponds to an interdomain spacing of 33.1 nm. As discussed above, these results are in good agreement with the estimated length for almost fully stretched PMPC₃₀-*b*-PDPA₆₀ copolymer chains.

As compared with former lamella films made from block copolymers, zwitterionic phosphorylcholine diblock copolymer systems offer a new option for the fabrication of lamellar structures in which one layer is biomimetic and nonfouling. In contrast to more conventional biocompatible hydrophilic polymers such as poly(ethylene oxide), the zwitterionic PMPC segment is insoluble in most organic solvents (except short chain alcohols). Consequently, PMPC-containing films can be manipulated under conditions that selectively affect the other block.

While this can surely be achieved with conventional systems too, the present case significantly expands range of possibilities in the macromolecular engineering field. In the case of biorelated applications in which the structural stability of lamellae in aqueous media is of interest, PMPC-*b*-PDPA films were found to very slowly disassembly in water to originate micelles. Therefore, additional stabilization strategies such as cross-linking chemistry applied to the PMPC block should be developed to facilitate the existence of these films in aqueous media on the long-term. Such investigations are under consideration and will be addressed in the near future.

CONCLUSIONS

The nanostructure of self-assembled copolymer films fabricated from a zwitterionic phosphorylcholine-containing pH-responsive PMPC₃₀-*b*-PDPA₆₀ diblock copolymer can be conveniently tuned by various film preparation protocols. Interesting copolymer morphologies induced by either solvent or thermal annealing were identified by SAXS and TEM studies.

AUTHOR INFORMATION

Corresponding Author

*E-mail: borsali@cermau.cnrs.fr. Telephone: 00 33 4 76 03 76 40. Fax: 00 33 4 76 03 76 29.

ACKNOWLEDGMENT

The authors acknowledge financial support from CNRS, RTRA Nanosciences-Grenoble, CNPq, CAPES (CAPES/CO-FECUB Grant No. 620/08) and the Federal University of Santa Catarina (UFSC). C.G. expresses thanks for financial support from CNPq through Grant No. 476703/2008-5. We thank Biocompatibles (Farnham, U.K.) for financial support, supply of the MPC monomer, and permission to publish these results. The European Synchrotron Radiation Facility (ESRF-France) and the Laboratório Nacional de Luz Síncrotron (LNLS-Brazil) are acknowledged for the provision of beam time. The authors thank Frédéric Charlot for his help for STEM observations at the Consortium des Moyens Technologiques Communs, INPG, Grenoble. This work was carried out at the Centre de Recherches sur les Macromolécules Végétales (CERMAV-CNRS), Grenoble-France.

REFERENCES

- (1) Segalman, R. A. *Mater. Sci. Eng. R.* **2005**, *48*, 191–226.
- (2) van Zoelen, W.; ten Brinke, G. *Soft Matter* **2009**, *5*, 1568–1582.
- (3) Smart, T.; Lomas, H.; Massignani, M.; Flores-Merino, M. V.; Perez, L. R.; Battaglia, G. *Nano Today* **2008**, *3*, 38–46.
- (4) Farrell, R. A.; Fitzgerald, T. G.; Borah, D.; Holmes, J. D.; Morris, M. A. *Int. J. Mol. Sci.* **2009**, *10*, 3671–3712.
- (5) Klok, H. A.; Lecommandoux, S. *Adv. Mater.* **2001**, *13*, 1217–1229.
- (6) Kuo, S. W. *Polym. Int.* **2009**, *58*, 455–464.
- (7) Bi, H.; Zhong, W.; Meng, S.; Kong, J.; Yang, P.; Liu, B. *Anal. Chem.* **2006**, *78*, 3399–3405.
- (8) Yoshimoto, K.; Hirase, T.; Madsen, J.; Armes, S. P.; Nagasaki, Y. *Macromol. Rapid Commun.* **2009**, *30*, 2136–2140.
- (9) Ishihara, K.; Takai, M. *J. R. Soc. Interface* **2009**, *6*, S279–S291.
- (10) Taktak, F. F.; Butun, V. *Polymer* **2010**, *51*, 3618–3626.
- (11) Lomas, H.; Du, J. Z.; Canton, I.; Madsen, J.; Warren, N.; Armes, S. P.; Lewis, A. L.; Battaglia, G. *Macromol. Biosci.* **2010**, *10*, 513–530.

- (12) Lomas, H.; Canton, I.; MacNeil, S.; Du, J.; Armes, S. P.; Ryan, A. J.; Lewis, A. L.; Battaglia, G. *Adv. Mater.* **2007**, *19*, 4238–4243.
- (13) Giacomelli, C.; Le Men, L.; Borsali, R.; Lai-Kee-Him, J.; Brisson, A.; Armes, S. P.; Lewis, A. L. *Biomacromolecules* **2006**, *7*, 817–828.
- (14) Hearnden, V.; Lomas, H.; MacNeil, S.; Thornhill, M.; Murdoch, C.; Lewis, A.; Madsen, J.; Blazas, A.; Armes, S.; Battaglia, G. *Pharm. Res.* **2009**, *26*, 1718–1728.
- (15) Mu, Q. S.; Zhao, X. B.; Lu, J. R.; Armes, S. P.; Lewis, A. L.; Thomas, R. K. *J. Phys. Chem. B* **2008**, *112*, 9652–9659.
- (16) Shen, L.; Du, J. Z.; Armes, S. P.; Liu, S. Y. *Langmuir* **2008**, *24*, 10019–10025.
- (17) Giacomelli, C.; Schmidt, V.; Borsali, R. *Langmuir* **2007**, *23*, 6947–6955.
- (18) Du, J. Z.; Tang, Y. P.; Lewis, A. L.; Armes, S. P. *J. Am. Chem. Soc.* **2005**, *127*, 17982–17983.
- (19) Almdal, K.; Koppi, K. A.; Bates, F. S.; Mortensen, K. *Macromolecules* **1992**, *25*, 1743–1751.
- (20) Ma, Y. H.; Tang, Y. Q.; Billingham, N. C.; Armes, S. P.; Lewis, A. L.; Lloyd, A. W.; Salvage, J. P. *Macromolecules* **2003**, *36*, 3475–3484.
- (21) Narayanan, T.; Diat, O.; Bosecke, P. *Nucl. Instrum. Meth. A.* **2001**, *467*, 1005–1009.
- (22) Hammersley, A. P. FIT2D: An Introduction and Overview. ESRF Int. Rep., ESRF97HA02T, 1997.
- (23) Simon, J. P.; Arnaud, S.; Bley, F.; Berar, J. F.; Caillot, B.; Comparat, V.; Geissler, E.; de Geyer, A.; Jeantey, P.; Livet, F.; Okuda, H. *J. Appl. Crystallogr.* **1997**, *30*, 900–904.
- (24) Iwata, R.; Suk-In, P.; Hoven, V. P.; Takahara, A.; Akiyoshi, K.; Iwasaki, Y. *Biomacromolecules* **2004**, *5*, 2308–2314.
- (25) Hua, F.; Ruckenstein, E. *Macromolecules* **2003**, *36*, 9971–9978.
- (26) Ahn, J. H.; Zin, W. C. *Macromol. Res.* **2003**, *11*, 152–156.
- (27) Viville, O.; Leclère, P.; Deffieux, A.; Schappacher, M.; Bernard, J.; Borsali, R.; Brédas, J.-L.; Lazzaroni, R. *Polymer* **2004**, *45*, 1833–1843.